Computation of the Unsteady Loading on a Fan Blade Due to Inlet Distortion Using Body Force Methodology

Younes Bouhafid, Thomas Berthelon

COMPUTATION OF THE UNSTEADY LOADING ON A FAN BLADE DUE TO INLET DISTORTION USING BODY FORCE METHODOLOGY

Younes Bouhafid
Graduate Research Assistant, ONERA
Email: younes.bouhafid@onera.fr

Thomas Berthelon
PhD, ONERA
Email: thomas.berthelon@onera.fr

ABSTRACT

The latest aero-propulsion configurations are characterized by a strong aerodynamic interaction between the engine and its environment. This interaction results in unsteady loads perceived by the fan leading to vibrations. In order to ensure the mechanical integrity of the blades, engine designers must evaluate these vibration levels very early in the design phases. To do so, the classic solution consists in running full-annulus U-RANS calculations to compute unsteady loading on the blade and then deduce the fan's forced response. However, such method can be computationally expensive and is consequently not adapted for large parametric studies conducted during the design phase of a blade. This paper presents a new method for calculating the forced response of a fan based on the use of body force calculations, which has a significantly lower computational cost compared to bladed U-RANS calculations. The main idea of the body force method is to replace the blades by source terms in the Navier-Stokes equations inside the volume swept by the fan. First, the application framework of the method is detailed. Then, the key step of the method which consists in computing the generalized aerodynamic forces from a body force calculation is presented and where the main idea involves concentrating the body force terms on the blade camber surface. A validation of the method is then proposed using a comparison with high fidelity U-RANS calculations for a BLI-like inlet distortion. It is found that the body force methodology reproduces the harmonic content of the computed generalized aerodynamic forces with a relatively good accuracy. Finally, an example of use of this method in a design context is presented as new body force calculations are run for two other inlet distortions that can occur in the takeoff phase: the ground vortex and the inlet flow separation.

NOMENCLATURE

G_{af} Generalized aerodynamic force
q Generalized coordinates vector
x Displacement vector
F_a Aerodynamic force
Ω Fan rotation speed
ω Modal pulsation
p Static pressure
Φ Eigenmodes matrix
ϕ Eigenvector
δ Deviation angle
δ_0 Deviation angle at maximum efficiency
β Relative flow angle
w Relative velocity vector
H Local distance between two blades
e Local thickness of a blade
N_{blades} Fan number of blades
M_{rel} Relative Mach number
f_n Normal component of the body force term
f_p Parallel component of the body force term
C_f Skin friction coefficient
θ Tangential coordinate
r Radial coordinate
W Mass flow rate

INTRODUCTION

Today, it is crucial for the aviation industry to significantly reduce its environmental impact. Reducing CO2 emissions requires improving the propulsive efficiency of aircraft. Achieving this objective requires the development of new propulsion architectures such as ultra high bypass ratio (UHBR) engines or boundary layer ingestion (BLI) configurations. These new configurations are characterized by a strong aerodynamic interaction between the fan and its environment. The resulting unsteady aerodynamic loading causes the blades to vibrate. This phenomenon is called forced response. Vibration levels that are too high can even lead to mechanical failure of the structure, due to fatigue phenomena. Engineers must therefore evaluate the vibration level of the blades very early in the design phase to avoid costly redesigns at the end of the design process.

Numerous numerical studies concerning the forced response of the fan caused by an inlet distortion have been carried out in the last decades. One can notably quote the study of Chiang [1] in which the authors evaluate the vibratory levels of a fan with a quasi-three-dimensional Euler code. Brerard [2] studied the forced response of a low aspect-ratio transonic fan due to different inlet distortions. The problem of forced response due to vortex ingestion has been studied on high bypass ratio engines by Green [3], Di Mare [4] and Berthelon [5]. Boundary layer ingestion concepts, which have become increasingly popular in recent years, are characterized by problems of forced response. Bakhle [6] details the design of a distortion-robust fan in this configuration. In most of the studies cited above, the estimation of vibration levels is based on the superposition principle, which assumes that it is possible to separate the aerodynamic forces related to motion and the aerodynamic forces related to distortion. This assumption is valid in many cases of turbomachinery [7–9]. The determination of the aerodynamic forcing is classically done by a U-RANS calculation of the whole fan stage. The unsteadiness of the calculation comes from the fact that the inlet distortion is fixed in the absolute reference frame, while the fan is rotating. A numerical transient is necessary before reaching the periodic regime of interest. Moreover, such a calculation requires to mesh all the blades of the fan, which leads to relatively large meshes. These calculations are relatively expensive, and therefore are only used occasionally in the design phases. A previous study [5] proposes an analytical model to calculate unsteady aerodynamic loading at very low cost. This model, in spite of very strong assumptions, seems to transcribe good trends in the case of vortex ingestion. Nevertheless, it is restricted to the swirl distortion and hardly applicable to other types of inlet distortion (BLI, crosswind separation...). The method presented in this work aims to be much more general while keeping a low cost compared to U-RANS methods. The idea of the method is to use body force calculations to extract the aerodynamic loading.

The body force method was originally proposed by Marble [10] in 1964. The main idea is to replace the fan by the volume swept by the blades during a complete rotation and in which source terms are imposed to the Navier-Stokes equations. This approach has since been improved and adapted to address fan design problems. In his thesis, Peters [11] studied numerically the impact of the interaction between the fan and the inlet on the performance of the engine using an improved body force model he derived from Gong's model [12], taking into account blade lean effects and blade losses at off-design operating conditions. Thollet [13], with his body force model based on a Lift/Drag analogy and using Kotapalli's [14] body force modeling of metallic blockage, showed in his thesis that his model correctly captures the effect of decreased intake length on flow separation delay on the intake lip. Godard [15] presented a body force methodology for fan blade design under distorted conditions. In his study, Godard showed that body force calculations have significantly smaller restitution time compared to classic U-RANS calculations, with a difference of two orders of magnitude. Godard [15] applied his methodology to conduct a parametric study based on variations of profile chord, blade leading edge angle and blade trailing edge angle. Defoe [16], based on Peters' [11] work, proposed a body force method using Hall's [17] model to compute the unsteady loading on a blade for vertically and radially stratified inlet distortions. To the knowledge of the authors of this paper, Defoe's paper is the only one to deal with structural loading using the body force method. The present paper, although inspired by Defoe's work, proposes a modal approach for structure adapted to the forced response phenomenon of the fan. Moreover, the results obtained with the presented body force methodology are compared to high fidelity U-RANS calculations.

This paper is organized in four parts. First, a brief presentation of the framework behind the study of the forced response of a mechanical structure is made. Second, the body force methodology for the computation of the generalized aerodynamic forces is described. Third, this methodology is applied for a test case emulating a BLI-type distortion and compared to the results obtained with a high-fidelity bladed U-RANS computation. Finally, the body force methodology is used for the study of the forced response due to two other inlet distortion cases: the ground vortex and the flow separation.

FORCED RESPONSE FRAMEWORK

Structural modelling

The equation of the dynamics of a linear structure can be written in a general way as follows.

$$M\ddot{x} + D\dot{x} + Kx = F_a(x, \dot{x}) \tag{1}$$

With x the displacement vector, M the mass matrix, D the damping matrix and K the stiffness matrix. The vector F_a represents the aerodynamic forces acting on the structure. The matrices are

usually obtained by finite element modeling. In the case of complex geometry such as a fan blade, the system may have a large number of degrees of freedom. In this situation, it is common to use modal basis in order to drastically reduce the size of the problem. To do so, an eigenvalue analysis is performed on the equation without external forces and damping. The search for eigenvalues results in Eq. (2). The eigenvalues ω represent the pulsations of the system and the eigenvectors ϕ represent the modes of the structure.

$$(K-\omega^2 M)\phi = 0 \tag{2}$$

The displacement of the structure can then be expressed as a linear combination of the eigenmodes, see Eq. (3), where Φ is the matrix of the eigenmodes and q the vector of the generalized coordinates, i.e. the coefficients associated at each mode.

$$x = \Phi q \tag{3}$$

The projection of the Eq.(1) into the eigenmode basis leads to the modal equation of the dynamics :

$$\mu\ddot{q} + \beta\dot{q} + \gamma q = G_{af}(\Phi q, \Phi\dot{q},) \tag{4}$$

By construction, the generalized mass matrix $\mu = \Phi^T M\Phi$ and the generalized stiffness matrix $\gamma = \Phi^T K\Phi$ are diagonal. Under Basile's hypothesis, the generalized damping matrix $\beta = \Phi^T D\Phi$ is also diagonal. It is then possible to separate the different modes. The generalized coordinate associated to the i^{th} mode is given by the following equation:

$$\mu_i\ddot{q_i} + \beta_i\dot{q_i} + \gamma_i q_i = G_{af,i} \tag{5}$$

The term of generalized aerodynamic forces of the mode i, $G_{af,i}$, corresponds to the projection of the aerodynamic forces on the modes, which gives under matrix notation :

$$G_{af,i} = \phi_i^T F_a \tag{6}$$

Decoupled approach

In order to solve the Eq. (5), it is common to use the principle of superposition which consists in separating the generalized aerodynamic force term into a motion-dependent part $G^d_{af,i}$ and forcing term $G^f_{af,i}$ dependent to the distortion but independent of the motion :

$$G_{af,i} = G^m_{af_i}(q_i, \dot{q_i}) + G^f_{af,i} \tag{7}$$

The damping generalized aerodynamic forces are assumed linear with the displacement and the velocity. This assumption is generally valid for turbomachinery blades which are of high density and stiffness and vibrate at low amplitudes. Finally, the displacement of the blades is described by the Eq.(8) where A is the aerodynamic stiffness matrix and B the aerodynamic damping matrix [1].

$$\mu\ddot{q} + \beta\dot{q} + \gamma q = Aq + B\dot{q} + G^f_{af} \tag{8}$$

In the case of a fixed distortion in the absolute reference frame, the aerodynamic forcing is periodic with a period of $T_{rot} = 2\pi/\Omega$ where Ω corresponds to the rotation speed of the fan. The G^f_{af} term can then be decomposed into a Fourier series as shown in Eq. (9).

$$G^f_{af} = \sum_k \hat{G}^f_{af,k} e^{jk\Omega t} \tag{9}$$

The linearity of the equation Eq.(8) allows to solve each harmonic independently. The generalized coordinate associated to the harmonic k, $\hat{q}_k$, is then obtained by Eq.(10).

$$\hat{q}_k = \frac{\hat{G}_{af,k}}{\gamma - A - (k\Omega)^2\mu + jk\Omega(\beta - B)} \tag{10}$$

In a design phase it is common to neglect A because this term is generally very small compared to γ. Moreover, the damping terms, β and B, only participate at the resonance, i.e. when the excitation frequency is close to the modal frequency ($k\Omega \sim \omega = \sqrt{\gamma/\mu}$). Outside the resonance zone, the modal amplitude associated with the k^{th} harmonic can then be approximated by Eq.(11).

$$|\hat{q}_k| = \frac{|\hat{G}_{af,k}|/\mu}{|\omega^2 - (k\Omega)^2|} \tag{11}$$

The idea of the method developed in this work is to use a body forces calculation in order to evaluate at a very low cost the $\hat{G}_{af,k}$ term.

GENERALIZED AERODYNAMIC FORCES COMPUTATION

The objective of this section is to detail the calculation of generalized aerodynamic forces in the case of a fan subjected to an aerodynamic inlet distortion.

[1] The index i is omitted for clarity.

Bladed approach

The calculation of the aerodynamic forcing most often involves a calculation of the entire wheel in the presence of the distortion. This one is classically imposed by using a fixed boundary condition in the absolute reference frame. Due to the rotation of the fan, the problem is unsteady. The temporal generalized aerodynamic forces are then obtained by projecting the aerodynamic forces at each time step on the mode as illustrated by the following equation:

$$G_{af}^{f}(t) = \int_S -p(t)(n.\Phi)dS \tag{12}$$

where n is the outward normal to the surface S of the blade.

Body force approach

All body force models rely on one key idea: replacing the volume swept by the fan by a domain where source terms are imposed. For this purpose, most body force models require a calibration process, usually through reference CFD results, to compute the source terms [11–13] inside the body force domain. In a design phase, it is preferable to keep calibration as light as possible. It is for this reason that Thollet's [13] improvement of Hall's [17] model has been chosen for the methodology developed in this paper.

Thollet's reformulation of Hall's model is given by:

$$f_n = K_M \frac{1}{2} w^2 2\pi \frac{\delta}{hb} \tag{13}$$

$$f_p = \frac{1}{2}\frac{w^2}{hb}(2C_f + 2\pi K_M(\delta - \delta_0)^2) \tag{14}$$

where:

$$h = \frac{H}{cos(\beta)} \tag{15}$$

H is the local distance between two blades along the tangential direction, w the relative fluid velocity vector, β the relative flow angle and δ the deviation angle. f_n and f_p are respectively the normal and the parallel component of the body force term f with respect to w. b is the blockage factor defined as $b = 1 - \frac{e}{H}$ with e the local thickness of the blade and is used to model the metallic blockage phenomenon. f_n models the blade loading due to pressure forces and f_p the different losses occurring in the flow. Such model is based on an analogy with the lift and the drag forces experienced by a thin airfoil. K_M is a function of the relative Mach number M_{rel} modelling compressible effects and based on Prandtl-Glauert corrections for subsonic flows and Ackeret corrections for supersonic flows:

$$K_M = \begin{cases} min(\frac{1}{\sqrt{1-M_{rel}^2}}, 3) & \text{if } M_{rel} < 1 \\ min(\frac{4}{2\pi\sqrt{M_{rel}^2-1}}, 3) & \text{if } M_{rel} > 1 \end{cases} \tag{16}$$

C_f is the skin friction coefficient and can be computed through calibration to match reference data or defined analytically with empirical correlations. We choose $C_f = 0.0592 Re_x^{0.2}$, which is the skin friction coefficient for a thin plate. δ_0 is the deviation angle of a body force calculation at nominal operating point for a given engine speed and models off-design losses. It is the only parameter requiring calibration. However, this calibration process is light as it requires only one body force calculation for each speed line as long as we know the nominal point position for a given regime.

The main idea behind Hall's body force modelling is to dilute the blade loading between two blades along the direction normal to the relative velocity w. A body force field is thus obtained. To obtain a force per unit area, Defoe's [16] approach is used and consists in proceeding in the opposite direction: the body force term is reconcentrated along the same direction. The force per unit area $f_{A_{\text{bf}}}$ on the blade camber surface is thus defined as:

$$f_{A_{\text{bf}}} = -\rho f_n \left(b \frac{2\pi r}{N_{blades}} cos(\beta) \right) \hat{n} \tag{17}$$

where $\hat{n}$ is the unit vector perpendicular to w and N_{blades} is the number of blades in the fan. Only the normal component f_n is used as it contains the effect of pressure forces on the blade. Since the body force methodology models the effect of the blades on the flow, a minus sign is required to compute the loading of the flow on the camber surface.

To compute the generalized aerodynamic forces, it is necessary to know the mechanical modes ϕ on the camber surface. Finite elements calculations are then performed to compute those modes for a given blade geometry. The results are then interpolated on the camber surface mesh using radial basis function (RBF) interpolation methods which are relevant for the interpolation of the unstructured finite elements mesh data on the structured CFD mesh of the camber surface. It should be noted that the mechanical modes are computed on the whole blade geometry and are interpolated only on the blade camber surface. This can be justified under the assumption of a thin blade: the mechanical modes variations along the blade's thickness are negligible.

Knowing the mechanical mode on the blade camber grid, the generalized aerodynamic modes of the i-th mode ϕ can be

computed:

$$G_{af}^{f} = \iint_{S_{cb}} (f_{A_{\text{bf}}} \cdot \phi) dS \tag{18}$$

where S_{cb} is the blade camber surface. The body force field vector f computed with a steady RANS calculation is a function of the three cylindrical coordinates: x, r and θ. Using Eq. (17), its possible to define a body force blade loading on each grid point of the body force domain. Thus, knowing the position of the blade with time and using a quasi-steady hypothesis, the unsteady loading on the blade camber surface can be computed. Mathematically, the unsteady loading is obtained with the parametrization of the coordinate θ with respect to time:

$$f_{A_{\text{bf}}}(x,\ r,\ \theta) = f_{A_{\text{bf}}}(x,\ r,\ \Omega t + \theta_0(x,r)) = f_{A_{\text{bf}}}(x,\ r,\ t) \tag{19}$$

where Ω is the angular velocity of the fan and $\theta_0(x,r)$ a dephasing term depending on the blade geometry and taking into account that the blade camber surface grid points do not necessarily have the same tangential coordinate θ. Physically, it is as if a virtual blade camber surface was rotating inside a non-axisymmetric pressure field inside the body force domain. As a consequence, the generalized aerodynamic force G_{af}^{f} in Eq. (18) will also be a function of time.

EVALUATION OF THE METHOD

Test Case

This section presents the results of the application of the body force method for the estimation of the aerodynamic loading on a given fan geometry representative of UHBR configurations. The mechanical model consists of a finite element model including the blade root. The degrees of freedom associated with the interface with the disk are clamped. The modes were computed numerically with the finite elements software NASTRAN. The first three modes studied in this work are shown in Fig 1. In order to compute generalized aerodynamic forces, these modes are interpolated on the camber surface using RBF interpolation with the library Scipy.

For both the body force computation and the bladed computation, numerical solution is obtained through the finite volumes code elsA [18]. Spatial integration is performed with Roe scheme. Smith k-L turbulence model is used to model Reynolds tensor [19]. As the body force solution is steady and the bladed solution unsteady, time integration is not performed with the same schemes for the two methods. Backward Euler scheme is used for steady computation. For the unsteady bladed calculations, a GEAR scheme is used with 10 subiterations.

The domain of the bladed computations is illustrated in Fig 2a. It includes the 18 blades of the fan. The mesh, generated with

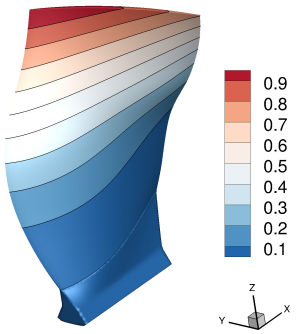

(a) 1F : first bending mode

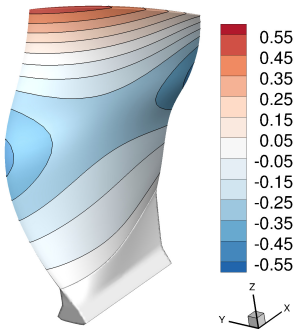

(b) 2F : second bending mode

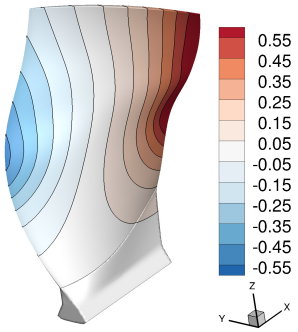

(c) 1T : first torsion mode

FIGURE 1: y-component of the three first mode shape.

NUMECA AUTOGRID, has 43 million cells. The body force calculation domain is shown in Fig 2b. The green part represents the body force volume where the source terms are applied. It was generated using an internal code and has 9 million cells. For both the body force and blades computations, the minimum wall distance is about 2 μm which results in $y_+ \approx 1$ using smooth flat-plate boundary layer theory for the different speed regimes studied in this paper. The outlet boundary conditions are set with

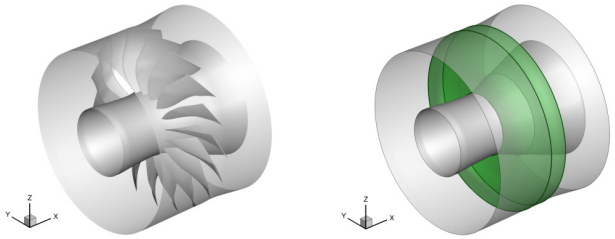

(a) Bladed (b) Body force

FIGURE 2: Computational domain

	Ω [rpm]	Pi_0 [Pa]	Ti_0 [K]
ground	2000	101325	288.15
flight	2680	33690	245

TABLE 1: Operating condition evaluated

a radial equilibrium defined by a pivot static pressure located at the hub. The inlet distortion is imposed by using a subsonic injection boundary condition, described by maps of total pressure, total enthalpy, direction vector and turbulent quantities. For unsteady calculations, an interpolation is performed to apply this condition in the absolute reference frame.

Steady comparison

Two operating conditions are considered in this study and are presented in table 1. The flight condition corresponds to a typical case of cruise flight, while the ground condition corresponds to a reduced regime when distortions related to the take-off can appear. In order to study the fan characteristics and the representativeness of the body force method, an iso-speed has been evaluated on these two operating conditions without distortion. For the bladed calculation, the iso-speed was performed on a single sector while the body force calculation was performed on an arbitrary azimuthal portion of 6 degrees. The stagnation pressure ratio and isentropic efficiency are shown in Fig. 3 and Fig. 4 as a function of the corrected flow rate W_c^* described in equation (20).

$$W_c^* = \frac{W \frac{\sqrt{Ti_0/288.15}}{Pi_0/101325}}{W_{c,ref}} \tag{20}$$

Regarding the stagnation pressure ratio, a very good agreement is obtained in the ground case, but discrepancies appear in the flight case. This is probably due to compressible effects, in

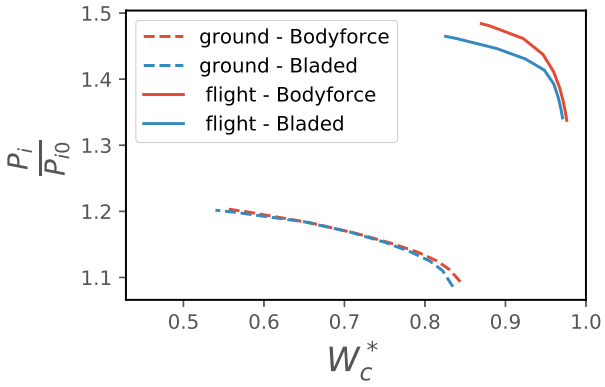

FIGURE 3: Comparison of stagnation pressure ratio between body force and bladed configuration.

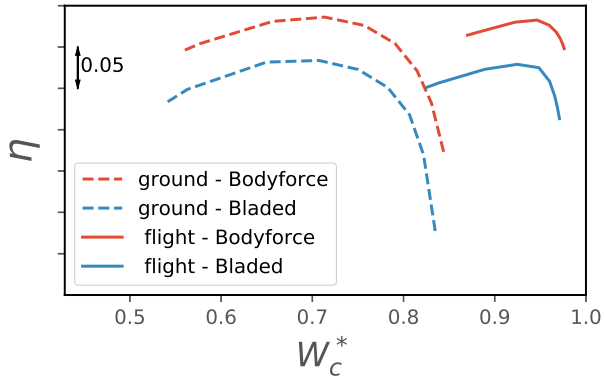

FIGURE 4: Comparison of isentropic efficiency between body force and bladed configuration.

particular the presence of shock at the blade tip which cannot be modeled in the body force formulation. Regarding the isentropic efficiency, the body force calculations show a good trend but overestimate the values in both cases. In order to improve these results, it is possible to calibrate the C_f term. More precisely, Hall's body force model is based on thin airfoil theory. As such, it does not take into account the flow losses due to shocks, flow separation and blade tip gap effects. One possible solution for the body force model to reproduce those losses could be to modify the C_f coefficient to match the bladed data. However, this is not the purpose of the method described here, which aims to require as little calibration as possible.

In order to better identify the causes of the observed discrepancies, a specific post-processing is used to extract the surface force applied to the bladed camber surface in the case of a bladed calculation, noted $f_{A_{\text{bl}}}$ and defined Eq. (21) where p_{ss} is

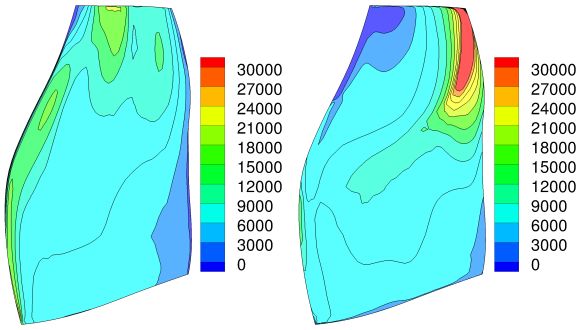

(a) Bladed (b) Body force

FIGURE 5: Component normal to the camber surface of $\vec{f}_A$ for the flight condition and the point of maximum efficiency.

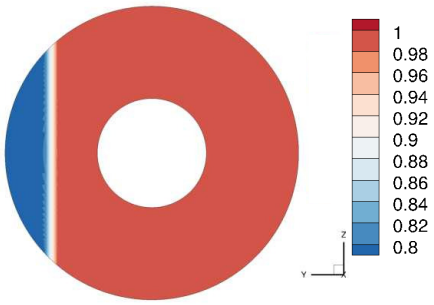

FIGURE 6: Stagnation pressure rate distortion map.

the pressure at suction side, p_{ps} the pressure at pressure side and n the normal of bladed camber surface.

$$f_{A_{\text{bl}}} = -(p_{ss} - p_{ps})n \tag{21}$$

The distribution of force per unit area is shown in Fig. 5 for the body force and the bladed case. Significant deviations are observed, especially in the upper part. The body force strongly overestimates the force at the trailing edge. Similar results have already been observed by Godard [15]. These discrepancies are attributed to the inability of the body force methods to capture the shocks. Even if the distribution is not very satisfying, the overall steady behavior (i.e. without distortion) remains acceptable.

Unsteady comparison

In order to evaluate the estimation of generalized aerodynamic forces using body force calculations, the stratified distortion in total pressure, shown in Fig. 6, was used. This kind of distortion is representative of a boundary layer ingestion configuration. Because of the stratified azimutal distorsion, the blade experiences a periodic unsteady loading as it rotates over time. U-RANS bladed calculations and body force calculations are run to estimate this loading in such condition. The U-RANS bladed calculations ran on 432 processors for 31 hours while the body force calculations ran on 90 processors for 2 hours, which indicates a CPU time ratio equal to 74.

Figure 7 shows the distribution of the harmonic content of the unsteady force per unit area f_A in bladed case and bodyforce cases. The first three harmonics are shown. As for the steady force, the bodyforce approach overestimates the levels at the trailing edge. These discrepancies are probably due to the incapability of the body force method to capture the shocks, and therefore the impact of a distortion on them. Nevertheless, these levels are only slightly higher than those observed at the leading edge in the bladed case. It seems that the intensity of the fluctuations is correctly reproduced but that their location is not. Moreover, the rapid decrease of the harmonic content as a function of the harmonic is very well captured by the bodyforce approach. The spatial-frequency content of the generalized aerodynamic forces distribution on the blade camber surface is plotted in Fig. 8 for the mode 1F. The harmonic content in terms of amplitude of the generalized aerodynamic forces distribution is obtained for the first three harmonics. Qualitatively, both the body force calculation and the bladed calculation indicate that the effect of the BLI-like distorsion can be felt at the top of the leading edge for the first flexion mode. However, as the observation of the harmonic content of the force per unit area f_A on the camber surface may suggest (see Fig. 7), the body force computations seem to notably overestimates the generalized aerodynamic forces distribution at the trailing edge. This overestimation can particularly be seen for the first harmonic $k = 1$ in Fig. 8b.

The harmonic content of the generalized aerodynamic forces of the first three mechanical modes is presented in Fig. 9. Despite the differences observed in the distribution of G_{af}, the harmonic content of the mode 1F shows a good agreement between the bladed computation and the body force computation. The amplitude and the global trend are well reproduced by the body force computation. Concerning the torsion mode 1T, the harmonic content is well rendered for the first three harmonics by the body force method while the global trend is in line with the result of the U-RANS bladed calculation. Finally, for the mode 2F, the body force significantly overestimates the amplitude of the first two harmonics. This can be problematic as it would lead to seriously overestimates the stress on the blade and lead to unnecessarily strengthening the blade during the design phase. Nonetheless, the amplitude of the last harmonics is well reproduced by the body force calculation while the global trend is satisfying.

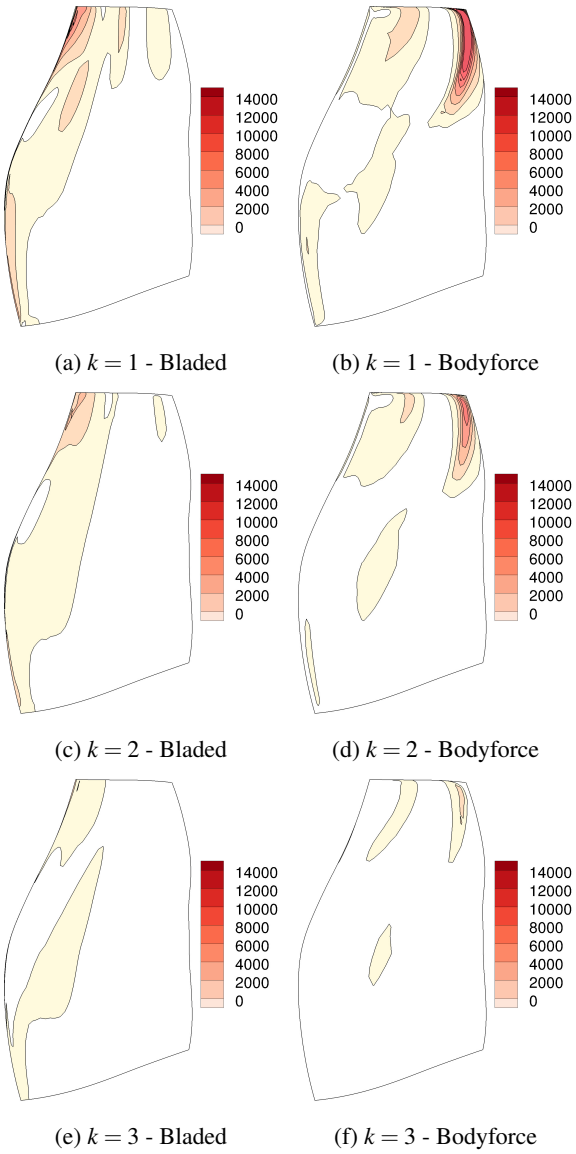

(a) $k = 1$ - Bladed (b) $k = 1$ - Bodyforce

(c) $k = 2$ - Bladed (d) $k = 2$ - Bodyforce

(e) $k = 3$ - Bladed (f) $k = 3$ - Bodyforce

FIGURE 7: Harmonic content of f_A distribution on camber surface.

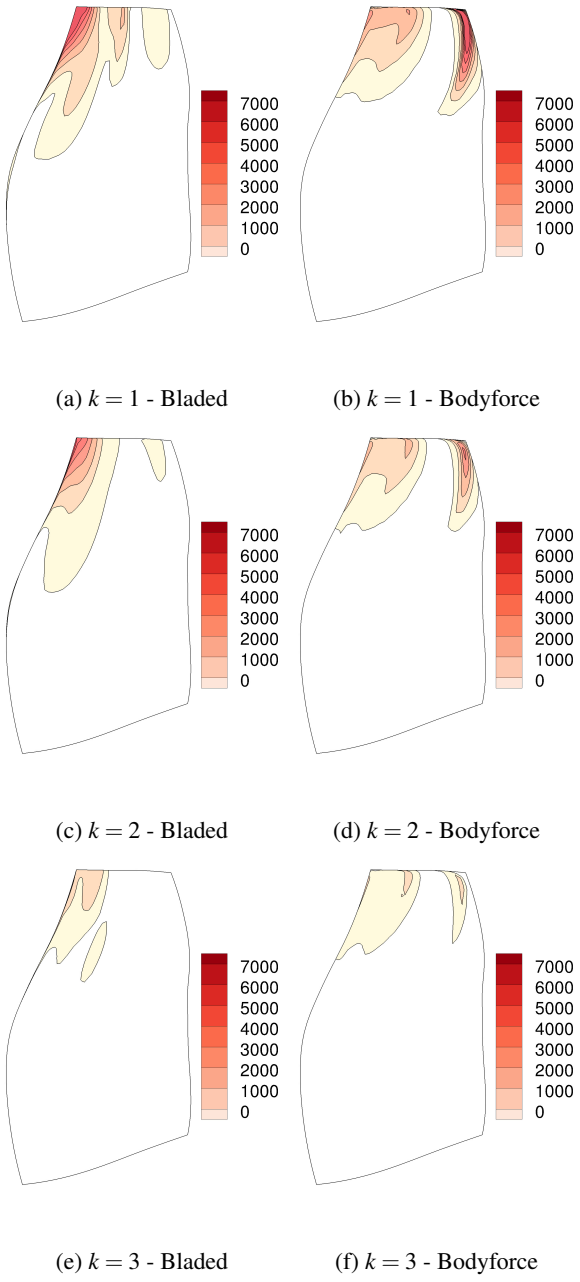

(a) $k = 1$ - Bladed (b) $k = 1$ - Bodyforce

(c) $k = 2$ - Bladed (d) $k = 2$ - Bodyforce

(e) $k = 3$ - Bladed (f) $k = 3$ - Bodyforce

FIGURE 8: Harmonic content of generalized aerodynamic forces distribution on camber surface for mode 1F.

APPLICATION ON OTHER DISTORTIONS

In this section, the method described above is used to evaluate the generalized aerodynamic forces generated by two distortions that can occur in the takeoff phases: the ground vortex and inlet flow separation. The conditions correspond to the ground conditions described in Table 1. Fig. 10a illustrates the case with ground vortex, through the visualization of non-dimensional total pressure map. The vortex is generated using the model of Vatistas [20] detailed in Eq. (22) in the frame relative to the center of the vortex.

$$v_t = \frac{\Gamma}{2\pi} \frac{r}{r^2 + r_c^2} \tag{22}$$

The circulation Γ is chosen at 50 m^2/s and the radius of the non-dimensional vortex is $r_c^* = \frac{r_c}{D} = 0.22$ where D is the fan

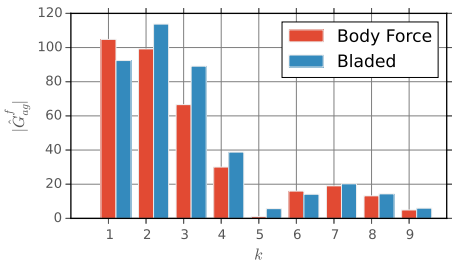

(a) mode 1F

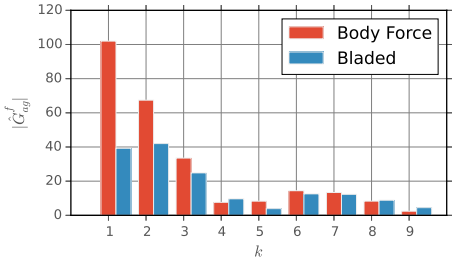

(b) mode 2F

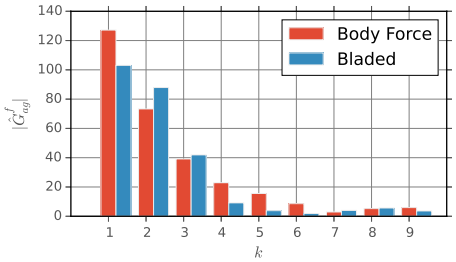

(c) mode 1T

FIGURE 9: Harmonic content of generalized aerodynamic forces for the first nine harmonics.

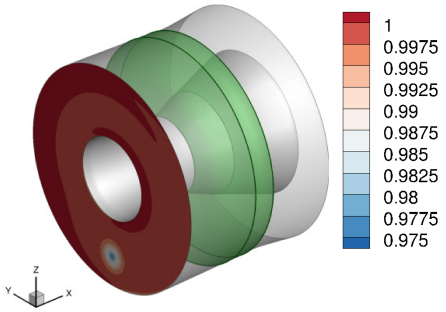

(a) Vortex case (non-dimensional total pressure)

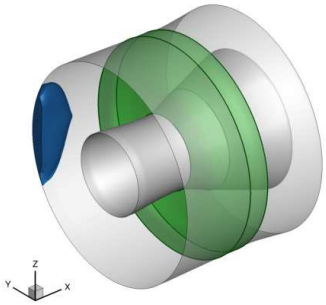

(b) Flow separation case (iso-surface of negative velocity along x axis)

FIGURE 10: Illustration of bodyforce computation with distortion near ground

diameter. The distortion is imposed through a subsonic injection boundary condition at the inlet.

For the separation case, the distortion is imposed through a mixed boundary condition, which consists in switching between a subsonic injection condition and a subsonic outlet condition according to the characteristic eigenvalues positiveness. Figure 10b shows the negative axial velocity isosurface which describes the recirculation zone.

In these two cases, the flow is not axisymmetric and therefore causes an unsteady load on the blades. Fig. 11 represents the frequency content of the G^f_{af} obtained for these two distortions. The appearance of the spectra is similar for the three modes and the two distortions: the amplitude decreases as a function of the harmonic. It should be noted that the relative amplitude between the two distortions is very different depending on the mode. Indeed, the levels are similar for the 2F mode while the vortex leads to levels much lower than those caused by the separation in the case of the 1F mode and the 1T mode. The proposed method thus allows to rank distortions at low cost.

CONCLUSION, DISCUSSION AND PERSPECTIVES

In this paper, a methodology to compute the unsteady aerodynamic loading of a fan due to the presence of distortion has been proposed. This method is a body force approach allowing a drastic reduction of the computational cost compared to the classical approach which consists in performing an unsteady computation of whole fan stage. Indeed, on the one hand the body force mesh is relatively light because the blades are not meshed, and on the other hand the problem becomes steady which simplifies its resolution. A factor of 70 is observed on the CPU time. The force field resulting from the body force calculation is post-processed in order to get the loading applied on the camber surface of the blade during its rotation. The projection of this loading on the deformation modes, also expressed on the camber surface of the blade, allows to obtain the temporal content of the generalized aerodynamic forces. These forces can then feed a linear dynamics calculation leading to the vibratory levels.

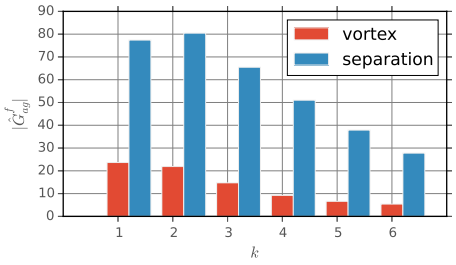

(a) mode 1F

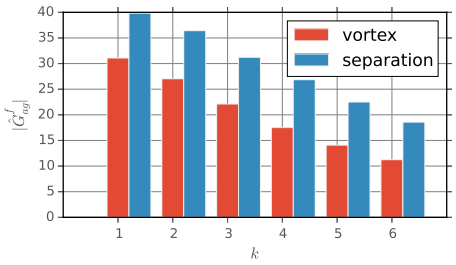

(b) mode 2F

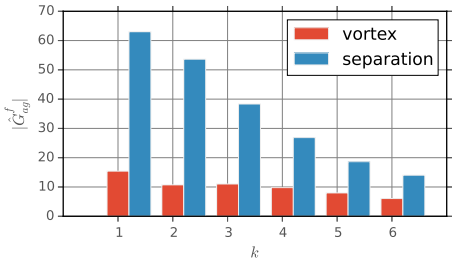

(c) mode 1T

FIGURE 11: Harmonic content of generalized aerodynamic forces.

The method has been evaluated on a case of boundary layer ingestion on a fan representative of a UHBR configuration. Although the local distribution of the forces differs significantly between the body force method and a classical calculation with a blade, the amplitudes of the frequency content of the generalized aerodynamic forces are relatively well captured for the three modes studied. The discrepancies in the distribution are particularly noticeable at the blade tip, where the compressible effects are most pronounced. The failure of the body force models in these areas with shock have already been highlighted [15]. Improvements of the body force model in this direction would allow a more accurate computation of the generalized aerodynamic forces.

The method was then used to compare two types of distortion that can occur during the takeoff phases: the ground vortex and the inlet separation. The comparison of the amplitude of frequency content shows that the inlet separation leads to higher levels than the ones induced by the ground vortex on the 1F and 1T modes, and similar levels for the 2F mode. This illustration shows the interest of this method in the design phases. Moreover, the body force model used requires almost no calibration, which is a very important point in the design phase.

The method explained in this paper allows to obtain an estimation of the aerodynamic forcing due to an aerodynamic distortion but does not allow to estimate the aerodynamic damping caused by the vibration. This parameter has a determining impact on the vibration levels obtained at a frequency coincidence. The estimation at low computational cost of the aerodynamic damping remains an open subject today.

REFERENCES

[1] Chiang, H.-W. D., and Kielb, R., 1993. "An analysis system for blade forced response".

[2] Bre´ard, C., Vahdati, M., Sayma, A. I., and Imregun, M., 2000. "An Integrated Time-Domain Aeroelasticity Model for the Prediction of Fan Forced Response due to Inlet Distortion ". *Journal of Engineering for Gas Turbines and Power,* ***124***(1), 02, pp. 196–208.

[3] Green, J., and Marshall, J., 1999. "Forced response prediction within the design process".

[4] di Mare, L., Simpson, G., and Sayma, A. I., 2006. "Fan forced response due to ground vortex ingestion". In Turbo Expo: Power for Land, Sea, and Air, Vol. 42401, pp. 1123–1132.

[5] Berthelon, T., Dugeai, A., Langridge, J., and Thouverez, F., 2019. "Analysis of vortex ingestion impact on the dynamic response of the fan in resonance condition". In Turbo Expo: Power for Land, Sea, and Air, Vol. 58684, American Society of Mechanical Engineers, p. V07AT36A010.

[6] Bakhle, M. A., Reddy, T., and Coroneos, R. M., 2014. "Forced response analysis of a fan with boundary layer inlet distortion". In 50th AIAA/ASME/SAE/ASEE Joint Propulsion Conference, p. 3734.

[7] Moffatt, S., and He, L., 2005. "On decoupled and fully-coupled methods for blade forced response prediction". *Journal of Fluids and Structures,* ***20***(2), pp. 217–234.

[8] Berthelon, T., Dugeai, A., Langridge, J., and Thouverez, F., 2018. "Ground effect on fan forced response". In Proc. of the 15th International Symposium on Unsteady Aerodynamics, Aeroacoustics and Aeroelasticity of Turbomachines, Vol. ISUAAAT15-094, American Society of Mechanical Engineers.

[9] Schmitt, S., Nürnberger, D., and Carstens, V., 2006. "Evaluation of the principle of aerodynamic superposition in forced response calculations". In *Unsteady aerodynamics, aeroacoustics and aeroelasticity of turbomachines*. Springer, pp. 133–144.

[10] Marble, F., 1964. Three dimensional flow in turbomachines, volume x of high speed aerodynamics and jet propulsion.

[11] Peters, A., Spakovszky, Z. S., Lord, W. K., and Rose, B., 2015. "Ultrashort nacelles for low fan pressure ratio propulsors". *Journal of Turbomachinery,* ***137***(2), p. 021001.

[12] Gong, Y., 1999. "A computational model for rotating stall and inlet distortions in multistage compressors". PhD thesis, Massachusetts Institute of Technology.

[13] Thollet, W., 2017. "Modélisations simplifiées de turbomachines pour l'analyse par la simulation des installations motrices complexes d'avions". PhD thesis, Toulouse, ISAE.

[14] Kottapalli, A. P., 2013. "Development of a body force model for centrifugal compressors". PhD thesis, Massachusetts Institute of Technology.

[15] Godard, B., De Jaeghere, E., and Gourdain, N., 2019. "Efficient design investigation of a turbofan in distorted inlet conditions". In Turbo Expo: Power for Land, Sea, and Air, Vol. 58554, American Society of Mechanical Engineers, p. V02AT39A011.

[16] Defoe, M., 2018. "Estimation of unsteady blade loading due to inlet distorsion using a body force rotor model".

[17] Hall, D. K., 2015. "Analysis of civil aircraft propulsors with boundary layer ingestion". PhD thesis, Massachusetts Institute of Technology.

[18] Cambier, L., Heib, S., and Plot, S., 2013. "The Onera elsA CFD software: input from research and feedback from industry". *Mechanics & Industry,* ***14***(3), pp. 159–174.

[19] Smith, B., 1994. "A near wall model for the k-l two equation turbulence model". In Fluid Dynamics Conference, p. 2386.

[20] Vatistas, G. H., Kozel, V., and Mih, W., 1991. "A simpler model for concentrated vortices". *Experiments in Fluids,* ***11***(1), pp. 73–76.